WATER RESOURCES RESEARCH, VOL. 31, NO. 5, PAGES 1273–1289, MAY 1995

Considerations for robust compositional simulations of subsurface nonaqueous phase liquid contamination and remediation

Sorab Panday,[1] Peter A. Forsyth,[2] Ronald W. Falta,[3] Yu-Shu Wu,[1] and Peter S. Huyakorn[1]

Abstract. A nonisothermal compositional model has been developed for examining nonaqueous phase liquid contamination and remediation scenarios. The governing mass balance equations and constraints have been presented, and various type of compositional formulations available have been examined. An efficient and robust formulation has been developed that addressed certain issues related to groundwater situations and overcomes numerical difficulties encountered with previous formulations. The proposed formulation collapses to that corresponding to the multiphase flow equation set when interface mass transfer is neglected. Numerical implementation of the formulation has been discussed, and example problems have been presented for benchmark and verification. The present formulation outperforms other currently used formulations for the isothermal case studied and performs at least as well as its counterparts for the nonisothermal case. Characteristics of the simulator that hinder convergence for difficult problems have been identified, and directions for even further improvements have been noted.

Introduction

Contamination of the subsurface environment by nonaqueous phase liquids (NAPLs) such as gasoline and other petroleum products and industrial wastes is a serious hazard to groundwater resources nationwide. The problem is compounded by the difficulty in characterizing the extent of contamination by the NAPL and by its components, which may dissolve in the water and volatize into the air phases. A critical step in understanding the impact of a subsurface release of NAPL is a modeling analysis of the NAPL migration and transport and fate of its crucial constituents. A fair number of numerical models of various levels of sophistication have been developed for assessing NAPL-contaminated sites. Vertical equilibrium, sharp-interface flow models were developed for quick preliminary investigations of spill extent and volume. Two-phase flow models examine migration of the NAPL phase after it has reached the water table. Three-phase flow models investigate NAPL flow in the unsaturated zone as well as its migration in the saturated zone. The three-phase simulators also find use in evaluating various pump-and-treat strategies for recovering free product (specifically, lighter than water NAPLs). Models with interface mass transfer of the NAPL component(s) determine the migration of its soluble chemicals with the groundwater or evaluate technologies such as water flooding as effective remedial measures. Three-phase flow models that incorporate air phase dynamics as well as interphase mass transfer, can also be used to evaluate the effectiveness of gas venting and air sparging as feasible remedial measures for contaminated sites. Finally, models that also include nonisothermal effects can examine the effectiveness of processes such as hot water flooding and steam injection as viable remediation schemes.

Typically, a site may undergo several remediation processes prior to closure. A variety of pump-and-treat systems and schedules may be developed followed by various enhanced remedial technologies. The efficiency and suitability of remedial measures depend on contaminant characteristics and site conditions. A model with sophisticated physical capabilities is therefore desirable for analyzing application of various remedial schemes at the site and for selecting suitable strategies and schedules leading to site closure. In addition, the model should automatically collapse to its simpler forms, when necessary, to ease the computational burden of a complete field analysis.

The goal of this work is to develop a practical tool for complete analysis of subsurface systems containing NAPLs (e.g., petroleum products and organic solvents). A comprehensive model has been discussed which utilizes the compositional approach for rigorous treatment of strongly coupled and highly nonlinear flow and transport situations. The formulation readily collapses to the much quicker multiphase flow scenario when interface mass transfer is neglected. The energy equation is included in the general formulation to handle nonisothermal scenarios, which merit consideration in examining potential remediation schemes that take advantage of the enhancement of flow and mass transport processes under thermal stimulation. The generality of the model further enables any number of phases to be present in the domain, thus reducing the problem if phases are absent in the system. Innovative numerical techniques are implemented to obtain robust, efficient, and accurate solution to the set of governing equations describing the various interactions of NAPL contaminants in the subsurface.

[1]HydroGeoLogic, Inc., Herndon, Virginia.
[2]Department of Computer Sciences, University of Waterloo, Waterloo, Ontario, Canada.
[3]Department of Geological Sciences, Clemson University, Clemson, South Carolina.

Paper number 94WR03288.
0043-1397/95/94WR-03288$05.00

Subject Review

Mechanisms that govern the subsurface behavior and fate of NAPLs have been investigated by many researchers, and mathematical models of various degrees of complexity have been established. Development of the governing equations describing multiphase flow and multicomponent transport in a porous medium dates back to the early 1960s, when the petroleum industry was interested in quantifying production and in evaluating the efficacy of secondary and tertiary oil recovery methods. A review of these equations, the various levels of complexity necessary for certain scenarios, and simplifications achieved by making practical working assumptions for various situations is provided by *Panday and Corapcioglu* [1989]. The compositional modeling approach provides the most rigorous representation of a multicomponent system for all perceivable contamination and remediation scenarios, particularly when nonisothermal effects are also included. However, because of the intensive computational burden of solving the strongly coupled compositional equations (one equation for each component), it is advantageous to solve the decoupled multiphase flow/multicomponent transport equations [*Reeves and Abriola*, 1988] for contaminants that are slightly soluble in water. Preliminary analyses may neglect the solubility effects and solve only for flow of the phases present in the system. Further simplifications to the governing equations can be made by treating the gas phase and NAPL as immobile, neglecting effects of temperature and composition on one or all fluid phases, neglecting capillarity effects, and finally invoking the vertical equilibrium assumption on flow behavior [*Huyakorn et al.*, 1992a].

A review of compositional models, the various formulations of the governing equations, constraints, interface mass transfer computation schemes, nonlinear numerical schemes, and matrix solution techniques is provided by *Corapcioglu and Panday* [1991]. Solution schemes evolved from implicit pressure–explicit saturation (IMPES) techniques (in which the pressure variable is solved fully implicitly with explicit updating of the saturation and composition terms within an iteration) to fully implicit techniques [*Aziz and Settari*, 1979] with various degrees and combinations of implicitness having been proposed for efficiency and robustness. *Forsyth* [1989] presents an adaptive-implicit technique which solves the equations fully implicitly only in zones where nonlinearities are high and applies the IMPES procedure in the rest of the reservoir to optimize robustness and efficiency. Newton-Raphson linearization is overwhelmingly the preferred technique of handling nonlinearities due to the quadratic convergence behavior, though quasi-Newton methods and their modifications are being investigated as competitive alternatives [*Nghiem*, 1983]. Optimal time step size control and techniques for improved accuracy have been discussed by *Todd et al.* [1972]. Large-sparse-block matrix solution procedures (such as Orthomin schemes) which outperform conventional banded or slice successive overrelaxation (SSOR) solvers have been discussed by *Behie and Vinsome* [1982]. Finally, techniques that take advantage of parallel and vector architecture are also a growing subject of investigations [*Chien et al.*, 1989]. This vast experience of the oil industry is invaluable for modeling NAPL contamination problems.

Numerical models of various levels of complexity have been developed to examine the subsurface migration of NAPL contaminants and their constituents. Multiphase flow models have been reported by *Forsyth* [1991], *Kaluarachchi and Parker* [1989], and *Faust* [1985], which are three-phase models that consider air as a passive phase. *Huyakorn et al.* [1994, 1992a] present a three-phase flow model that considers all phases as active but can reduce to various simpler forms when one or more phases are considered passive or absent. The component transport equation was incorporated in a decoupled manner by *Huyakorn et al.* [1992b]. Compositional models developed to examine groundwater contamination scenarios include those by *Abriola and Pinder* [1985], *Corapcioglu and Baehr* [1987], *Forsyth and Shao* [1991], and *Sleep and Sykes* [1993], with nonisothermal effects included by *Falta et al.* [1992], *Panday and Corapcioglu* [1994], and *Forsyth* [1994]. *Abriola and Pinder* [1985] present a two-dimensional (2-D) model with two NAPL components, one of which can transfer mass across phase boundaries. *Corapcioglu and Baehr* [1987] present a fully general formulation but solve the system in two dimensions with a residual NAPL saturation assumption. The models of *Forsyth and Shao* [1991], *Sleep and Sykes* [1993], and *Adenekan et al.* [1993] are more general in that no approximation is made regarding the various states of the system or the flow of the phases. A variable substitution scheme is presented that switches constraints and primary variables appropriately when phase transitions occur at any location in the modeled domain. Nonisothermal effects were included by *Panday and Corapcioglu* [1994] to analyze the freeze/thaw behavior of contaminated soils in Arctic regions, while *Falta et al.* [1992] and *Forsyth* [1994] include the thermal regime to examine the effects of hot water flooding or steam injection.

As compositional simulators were increasingly used to examine groundwater NAPL contamination scenarios, it became apparent that certain situations exist in typical contamination/remediation analyses which require special attention for robust accurate and efficient computations. Specifically, an inert gas phase, NAPL-free zones, and thermal simulations near the critical point of the fluids create extra difficulties not addressed in the petroleum literature. These issues are addressed herein to provide a more robust compositional formulation for examining NAPL contamination problems and to provide insight into the causes of the weaknesses of certain formulations, so that further research might provide even more robust simulators.

Governing Equations

The general three-dimensional macroscopic equation for transport of a species k in fluid phase l states that the rate of increase of mass of component k in phase l within a representative elementary volume (REV) is equal to the sum of advective and dispersive fluxes of component k in phase l into the REV and the mass transfer of component k to phase l from the other phases present in the REV. Thus the conservation equation for species k in phase l can be written as [*Corapcioglu and Panday*, 1991]:

$$\frac{\partial}{\partial t}(\phi \rho_l S_l \omega_l^k) = -\frac{\partial}{\partial x_i}(\rho_l V_{li} \omega_l^k) + \frac{\partial}{\partial x_i}\left(\phi \rho_l S_l D_{lij}^k \frac{\partial \omega_l^k}{\partial x_j}\right) + \Gamma_l^k + q^k \qquad (1)$$

where $x_i (i = 1, 2, 3)$ form an orthogonal coordinate system, t is time, k is the species component index (k = water (w), air (a), and components introduced by the NAPL (c, $c = 1, 2, \ldots, N_c$)), N_c is the total number of NAPL components, l

is the phase index (l = water (w), NAPL (n), and gas (g)), ρ_l is the density (mass/molar) of phase l, ω_l^k is the mass/mole fraction of species k in phase l, ϕ is the porosity of the medium, S_l is the saturation of phase l, D_{lij}^k is the hydrodynamic dispersion tensor in phase l (which includes mechanical dispersion of phase l and effective molecular diffusion of species k in phase l), Γ_l^k is the net rate of mass transfer into phase l within the REV, and q^k is a source term for component k. V_{li} is the Darcy velocity of phase l expressed as

$$V_{li} = -\frac{k_{ij}k_{rl}}{\mu_l}\left[\frac{\partial P_l}{\partial x_j} - \rho_l^m g \frac{\partial Z}{\partial x_j}\right] = -k_{ij}\tau_l \frac{\partial \psi_l}{\partial x_j} \qquad (2)$$

where k_{ij} is the absolute permeability tensor of the medium, k_{rl} is the relative permeability of phase l, μ_l is the dynamic viscosity of phase l, P_l is the pressure of phase l, ρ_l^m is the mass density of phase l, g is the gravitational acceleration, τ_l is the phase mobility, ψ_l is the total potential of phase l, and Z is the vertical coordinate direction. Constraints that apply to this system of equations are

$$\sum_k \omega_l^k = 1 \qquad l = w, n, a \qquad (3)$$

i.e., the sum of the mass/mole fractions of all components k within a phase equals unity, and

$$\sum_l S_l = 1 \qquad (4)$$

Constitutive relations that express flow behavior and the saturation-pressure state of the REV include relative permeability relationships for each fluid phase and the retention functions. The relative permeabilities of the phases are a function of phase saturations. For a water-wet system (typically encountered in groundwater contamination scenarios) the relative permeability of water is a function of water saturation, and the relative permeability of gas is a function of gas saturation, while relative permeability to NAPL is a function of all saturations. Three-phase relative permeabilities have been expressed by empirical relations (*Stone*'s [1973] formulas) and by three-phase extensions of network model expressions [*Kaluarachchi and Parker*, 1989]. Three-phase retention functions are also extrapolated from two-phase relations from wettability and interface considerations as used by *Forsyth* [1989], and two-phase retention functions for any fluid pair may be obtained from standardized two-phase curves by interfacial tension scaling [*Kaluarachchi and Parker*, 1989] if direct experimental data are unavailable. The physical and mathematical models that provide the constitutive relations for multiphase systems in a porous medium are discussed by *Panday and Corapcioglu* [1994]. They differ from the multiphase flow relations published in the oil industry owing to the presence of only air-water regions in a groundwater contamination scenario. The constitutive relations used in this work are provided by *Huyakorn et al.* [1994] and include a choice of network models, or empirical (Stone's) relations for relative permeabilities, and linear transition assumptions for the retention functions when pristine portions of the domain are invaded by NAPL.

The energy conservation equation within a porous medium, required for nonisothermal simulations, is expressed as

$$\frac{\partial}{\partial t}\left[\sum_l (\phi\rho_l S_l U_l) + (1-\phi)\rho_s U_s\right] = -\sum_l (h_l \rho_l V_{li}) + \sum_l \sum_k \frac{\partial}{\partial x_i}\left[\phi\rho_l S_l D_{lij}^k h_l^k \frac{\partial \omega_l^k}{\partial x_j}\right] + \frac{\partial}{\partial x_i}\left(\Lambda_{ij}\frac{\partial T}{\partial x_j}\right) + q_E \qquad (5)$$

where U_l is the internal energy of phase l; ρ_s and U_s are the density and internal energy of the soil solids; h_l and h_l^k are the enthalpies of phase l and of species k in phase l, respectively; Λ_{ij} is the overall porous medium thermal conductivity tensor; T is temperature; and q_E is the energy source term. The internal energy or enthalpy of a phase is a function of the phase composition and of the internal energies or enthalpies of the individual constituents. Densities and viscosities of the phases are functions of temperature, pressure, and composition of the respective phases. The effects of temperature, composition, and overburden on the retention functions [*Panday and Corapcioglu*, 1994; *Corapcioglu and Panday*, 1991] have been neglected in this study.

The compositional transport equation for each species k within the REV is obtained by summing (1) over all phases present, giving

$$\frac{\partial}{\partial t}\left[\phi\sum_l (\rho_l S_l \omega_l^k)\right] = -\sum_l \frac{\partial}{\partial x_i}(\rho_l V_{li}\omega_l^k) + \sum_l \frac{\partial}{\partial x_i}\left(\phi\rho_l S_l D_{lij}^k \frac{\partial \omega_l^k}{\partial x_j}\right) + q^k \qquad (6)$$

Under equilibrium conditions of phase partitioning, the mass transfer rate for component k into a phase equals the mass transfer rate out of it (i.e., $\Sigma_l \Gamma_l^k = 0$), and the mass/mole fractions of a component k within all phases are related by equilibrium thermodynamics.

The compositional transport equations (6) for all k species within the REV and the energy transport equation (5) (for nonisothermal cases) form the primary set of partial differential equations governing the fate of a contaminant within a porous medium system, with (2) expressing the flux of the phases. Additional equations include the mass/mole fraction constraints for each phase, the saturation constraint within the REV, the relative permeability functions, the capillary pressure functions, and the equilibrium partitioning relations. Details and derivations of the compositional transport equations and the necessary constraints are provided by *Corapcioglu and Panday* [1991] with additional considerations for groundwater systems being discussed by *Panday and Corapcioglu* [1994]. Solution to the highly nonlinear equation set is sought simultaneously for pressure and saturation distributions of the phases, the temperature distribution, and the mass/mole fractions of the species within all phases, at any time within the domain.

Multicomponent, multiphase models that incorporate kinetic mass transfer mechanisms are also a current topic of interest to the research community, since it is unclear whether the ideal equilibrium assumptions used in current models are suitable for certain situations. The disadvantage in these situations is that the number of primary unknowns is tripled for a three-phase analysis, and practical simulations become unfea-

sible. Conceivably, the techniques discussed in this work may be extended to kinetic mass transfer models as well. However, there may be several other numerical considerations involved. Another disadvantage of developing a kinetic mass transfer model is the current lack of quantification of even first-order mass transfer rates at any given temperature. Finally, accurate kinetic models should approach the correct equilibrium condition, which may deviate significantly from ideal conditions currently used. Further research should therefore focus on evaluating the accuracy of nonideal equilibrium calculations for groundwater contamination scenarios before increasing the complexity of computations required by kinetic models.

Discussion of Compositional Formulations

Various formulations have been used to solve the set of governing equations that describe the compositional model. Past research efforts in this direction have aimed at alleviating the numerical difficulties associated with petroleum reservoir simulations. In subsurface NAPL contamination and nonisothermal remediation situations, however, some additional difficulties arise, due to the presence of the air component, which is nonreactive and does not dissolve in either water or oil phases, and due to the presence of two-phase zones in the pristine portions of the subsurface, where NAPL is absent. The latter has been addressed in the multiphase flow simulator of *Huyakorn et al.* [1992a, b, 1994]. The presence of inert components (like air) alongside components that have significant mass transfer among phases (like steam, or highly volatile or soluble NAPL components) presents certain peculiarities, which should be addressed in choosing a compositional formulation as well as its numerical implementation.

The various published compositional formulations (see *Corapcioglu and Panday* [1991] for review) can be grouped into three basic categories, with variations within a category enabling quicker solution to specific scenarios. The first category (category A) involves methods of implementation of the compositional model, similar to the scheme detailed by *Coats* [1980]. The fundamental methodology involves assembling all the balance equations (5) and (6), as well as the constraints (3) and (4) into a Newton-Raphson linearized global coefficient matrix. Computational burden of a block matrix solution may be eased by reducing the block size by partial Gauss elimination over the constraint equations. This can be achieved since each of the constraints involves only one node for a fully lumped storage matrix. A suitable block solver may then be used to solve for the reduced set of unknowns, with back substitution providing the remaining eliminated variables. Full pivoting ensures a diagonally dominant set of variables.

Relevant highlights of this formulation are as follows.

1. Variable substitution of unknowns is not required, since all relevant equations are assembled. Only constraint equations are switched, depending on the state of the system at any node. This makes coding and debugging easier.
2. Large storage requirements are imposed by the simulator due to the assembly of constraints in the global matrix.
3. The computational burden per Newton iteration is also increased by the calculation of the Jacobian for the constraint equations and by the partial Gauss elimination on the constraints.
4. Pivoting always ensures optimal diagonal dominance as opposed to preselecting sets of primary variables as in the other categories, where one of the preselected secondary variables may actually have been a better candidate as a primary variable. This formulation therefore should not perform worse than the most optimally selected primary variables of the other categories in terms of Newton iteration count, for a similar total variable set (i.e., category B).

The second category of formulations (category B) is basically described by *Forsyth and Shao* [1991]. In this method the variables are separated into primary variables (solved for using the balance equations (5) and (6)) and secondary variables (solved for using the constraint equations (3) and (4)). The choice of primary variables, and their alignment to the balance equations, is crucial to robustness of the simulator. Switching of primary variables at any node may be performed to provide diagonally favorable matrix systems. The set of variables includes phase pressures P_l, phase saturations S_l, temperature T, and phase mole fractions of each component k, in any one phase l, (ω_l^k). Optimal assignment of these variables to the primary and secondary equations is discussed by *Forsyth and Shao* [1991], along with switching of variables and equations when the state of a node changes. Relevant steps for the selection of equations and variables at each Newton iteration are as follows.

From known primary variables calculate all secondary variables. The key to this scheme is that the choice of primary variables always allows calculation of P_n and P_w from p_c functions, since P_a and the relevant saturations are always a part of the primary variable set. This is done as follows.

1. Use saturation constraint to give the remaining unknown saturation.
2. Calculate P_n and P_w from all S_α, $\alpha = w, n, a$, and p_c, functions.
3. From known pressures, saturations, and some mole fractions, calculate the remaining mole fractions from mole fraction constraints, and equilibrium partitioning. If a phase is absent at any node ($S_l = 0$), the mole fraction constraint for phase l is not valid, and $S_l = 0$ replaces $\Sigma_l \omega_l^k = 1$. Further, in the primary variable set, ω_l^k replaces S_l, and any of the other component mole fractions which are defined in phase α are switched to the mole fraction in a different phase which is present at that location. Choice of phase in which these mole fractions are calculated is again critical to robustness of the simulator. In general, using gas phase mole fractions as primary variables provides the best robustness, since mass transfer of components to the gas phase is usually the largest.
4. Assemble all transport equations using Newton-Raphson linearization.
5. Solve for the primary variables.
6. Repeat above procedure until convergence and proceed to new time step.

Relevant highlights of this formulation are as follows.

1. If a noncondensible gas exists, it is necessary to leave some gas in place throughout the domain, since switching criteria are not available for variable substitution. Furthermore, the Jacobian becomes singular if noncondensible gas saturation becomes identically zero.
2. For a noncondensible gas case, negative mole fraction is a possible solution, and a penalty source term is required.
3. With condensible gas, the aforementioned difficulties are resolved, but computations are less robust, especially when extremely low partitioning is provided to an almost noncondensible gas situation, to force the simulation to proceed.
4. The computation sequence shown above is efficient. Sec-

ondary variables can always be calculated in a one-step procedure.

5. The number of secondary variables is less than that for the Z formulation (see categories C and D that follow).

6. Variable substitution requires the entire set of ω variables to be switched depending on phase transitions.

The third category of formulations (category C) involves solving for Z^k, the mole/mass fraction of component k within all phases in the void volume, as the primary variables. The advantage of this formulation is that its solution is bounded and that a flash package may easily be attached to it to provide all other variables. The relation between the Z formulation and the conservation equations (6), is discussed by *Corapcioglu and Panday* [1991], who also examine implementation of the Z formulation.

Relevant highlights of this formulation are as follows.

1. Variable substitution is not required because all the Z^k are always primary variables.

2. The formulation can handle cases with noncondensible gas, since the flash package should be sophisticated enough to return physically realizable solutions.

3. Matrix stiffness is not obviously affected for a noncondensible gas case, so its robustness should not be vastly different from its condensible gas case.

4. Newton iterations are required for secondary variables in the flash calculation. This is a lot more computationally intensive than eliminating secondary variables using a one-step procedure as in category B. If a full matrix is assembled as in category A, both storage and time of computation are more.

5. The Z formulation shifts numerical difficulties (that would arise as a result of low air saturations for a noncondensible air system) to the flash package. Saturation and pressure calculations could encounter serious truncation errors at low saturations. This, in turn, affects the flow field in the transport equations at each iteration, causing instabilities in the convergence behavior.

6. Newton convergence may be destabilized further in the Z formulation because of a poor Jacobian matrix, caused by slope discontinuities and branch calculations of a flash package intended to provide physically meaningful solutions.

The scheme used in the present work (category D) combines the most visible advantages of the various compositional formulations to provide optimal robustness and efficiency for solution to a wide variety of groundwater contamination scenarios. The primary disadvantage of the formulation in category A is its large computer storage and time requirements for assembly and simultaneous solution of all constraint equations in the global matrix. The scheme is thus inappropriate for developing a simulator that may be used on workstations or minicomputers. The adopted scheme combines a variation of the variable substitution scheme of category B with the Z formulation of category C. Air pressure and the relevant saturations are still primary variables as in category B, but the remaining primary variables are the Z^k of certain components (void-volume mole fractions) as opposed to ω_l^k (the phase mole fractions in any one specific phase l). Figure 1 provides the alignment of equations to unknowns, and supplies all secondary equations required to completely characterize the variables for a node containing all three phases. A derivation of these Z equations is provided in the next section. The present formulation solves for the primary variables using the primary equations (A and B in Figure 1), after which the secondary variables are updated using equations C through K in Figure 1 successively, at each Newton iteration. Selection of primary variables is such that all secondary variables can be calculated in a one-step procedure, with not more than four (two for most cases) iterations over equations E through J in Figure 1 being required within any Newton iteration to resolve the mild nonlinearity between liquid phase densities and their mole fractions. A 2×2 or 3×3 inversion is required on equations G in Figure 1, if two or three phases respectively, are present at the node. The variable substitution scheme for primary variables is as follows: If a phase disappears at a node within any iteration, the primary variable $S_l (l = a, n)$, of the phase that disappears, is replaced by Z^k for a component k that has l as its "master phase." (The master phase of a component is generally chosen as the natural state of the component at reference pressure and temperature conditions.) If water phase disappears from a node, S_a is replaced by Z^w as the primary variable. In addition, the secondary equation $\Sigma_k \omega_l^k = 1$ is no longer valid for the absent phase (or phases) l and is replaced by $S_l = 0$. Further, the Z^k which replaces S_l as a primary variable is used to compute ω_l^k using equation F, which replaces the appropriate equation from H, I, or J. Phase l may reappear if $\Sigma_k \omega_l^k \geq 1$ at any later iteration, and the secondary equations and primary variables are switched back for the next iteration. In addition, if a noncondensible gas exists in the system, its appearance is denoted by $Z^K > 0$ for incondensible component K. This system of phase switching is performed, depending on whether one, two, or three phases exist at any location. It should also be noted that the logic provided above for a noncondensible, nonreactive gas can be applied to any inert component in any phase, which does not transfer mass to other phases.

Relevant highlights of our proposed formulation are as follows.

1. Variable substitution (almost the same as for category B) is required. However, unlike scheme B, switching criteria are available for variable substitution, if inert components are present in the system. This is because if an inert component is present at any location (calculated as $Z^k > 0$ in any Newton iteration), it can be present only if the master phase of that component has arrived.

2. Variable substitution involves replacing S_l by a Z^k when phase l saturation goes to zero. The variable substitution of ω_g^k to ω_n^k, etc., does not occur here, as in category B. Fewer variables being switched introduces less oscillations to the system between Newton iterations, in addition to being easier to code.

3. The matrix is diagonally stable for noncondensible gas case, since the accumulation term is proportional to $Z^K \Sigma_\alpha \rho_a S_\alpha$. (Details are given in the next section.)

4. Secondary variables can be calculated directly, and Newton iterations are not required as in the flash calculation of the original Z formulation. The relatively mild nonlinearity of density with phase mole fractions of the components is easily resolved within two iterations for most cases. Time lagging this nonlinearity slows down the Newton convergence, and it is always best to provide as exact a Jacobian as possible for robustness and overall increase in computational speed.

5. More secondary variables occur than would for method B, but that should be offset by the above advantages over method B.

6. All the advantages of method B over method A are incorporated here with respect to solution speed and storage demands. The disadvantages of method B (primarily the switching criteria for low/no-phase-transfer systems and near singularities of the Jacobian) have also been eliminated here,

Equations	Variables
Primary equations and unknowns	
A. Mass balance equations for components 1 to NC. (Components NC-2 to NC have, as master phases, air, NAPL, water respectively).	P_a, S_a, S_n, Z^k; k = 1...NC-3
B. Energy Balance	T
Secondary equations and unknowns	
C. Saturation Constraint	S_w
D. p_c curve functions	P_w, P_n
E. $F_\ell = \frac{\rho_{m\ell} S_\ell}{\sum_\beta (\rho_{m\beta} S_\beta)}$; $\ell = n,w,a$	F_n, F_w, F_a; where $F_\alpha = \frac{mol_\alpha}{\sum_\beta mol_\beta}$; $\alpha,\beta = w,n,a$
F. $\omega_\ell^k = \frac{K_{\ell:M} Z^k}{\sum_\beta (F_\beta K_{\beta:M}^k)}$	ω_ℓ^k; ℓ = w,n,a; k = 1, NC-3
	ω_a^{NC-2} ; ω_n^{NC-1} ; ω_w^{NC}
G. $\sum_k \omega_\ell^k = 1$; $\ell = w,n,a$	
H. $\omega_\ell^{NC-2} = K_{\ell:a}^{NC-2} \omega_a^{NC-2}$; $\ell = w,n$	ω_ℓ^{NC-2} ; ℓ = w,n
I. $\omega_\ell^{NC-1} = K_{\ell:n}^{NC-1} \omega_n^{NC-1}$; $\ell = w,a$	ω_ℓ^{NC-1} ; ℓ = w,a
J. $\omega_\ell^{NC} = K_{\ell:w}^{NC} \omega_w^{NC}$; $\ell = a,n$	ω_ℓ^{NC} ; ℓ = a,n
K. $Z^k = \sum_\ell (\omega_\ell^k F_\ell)$; k = NC-2, NC-1, NC	Z^k, k = NC-2, NC-1, NC

Figure 1. Alignment of equations and variables for the case where all phases are present.

as are the disadvantages of method C. The computational sequence per iteration is more intensive than in method B for calculation of secondary variables but less intensive than for methods A and C. Larger stability should provide quicker convergence and allow larger time steps than for any of methods B or C, for all types of problems, including if inert components are present in the system.

Derivation of the *Z* Formulation and Its Secondary Variables

To use overall composition as the primary variable, the mole fraction of a fluid phase l is first defined as moles present in phase l per total moles present in the fluid phases occupying the voids,

$$F_\alpha = \left[\text{moles}_\alpha \Big/ \sum_{\beta=1}^{NP} \text{moles}_\beta \right]$$

where α and β are the phase indices, and NP is the total number of fluid phases in the system (note that F_α may be defined in terms of moles or mass).

Hence for any fluid phase $\alpha(\alpha = w, n, a)$, the mole fraction of a phase α is expressed by

$$F_\alpha = \frac{\rho_\alpha S_\alpha}{\sum_\beta \rho_\beta S_\beta} \tag{7}$$

By definition the summation of the mole fractions over all fluid phases gives

$$\sum_\alpha F_\alpha = 1 \tag{8}$$

and the mole fraction of each component k present in the total soil volume is

$$Z^k = \sum_\alpha (\omega_\alpha^k F_\alpha) \qquad k = 1, \cdots, NC \tag{9}$$

Substitution of ω_α^k in (9) with the equilibrium partitioning relation ($\omega_\alpha^k = K_{\alpha:\beta}^k \omega_\beta^k$) gives

$$Z^k = \sum_\alpha (F_\alpha K_{\alpha:M}^k) \omega_M^k \tag{10}$$

where subscript M denotes a master phase for component k, to which the component is referenced. Note that in (10), $K_{\alpha:M} = 1$ when $\alpha = M$; hence for each phase α, we obtain

$$\omega_\alpha^k = \frac{K_{\alpha:M}^k Z^k}{\sum_\beta (F_\beta K_{\beta:M}^k)} \tag{11}$$

Further, since the primary variables are Z^k instead of ω_M^k, one of the mass/mole fraction constraints may be replaced by

$$\sum_{k=1}^{NC} Z^k = 1 \tag{12}$$

which is the overall mass/mole fraction constraint for components k present in the voids.

To see the transformation of (6) to make Z^k a primary variable, consider the net rate of accumulation term, the first term on the left-hand side of (6). Substituting for ω_α^k with (11) gives

$$\phi \sum_\alpha (\rho_\alpha S_\alpha \omega_\alpha^k) = \frac{\phi Z^k \sum_\alpha (\rho_\alpha S_\alpha K_{\alpha:M}^k)}{\sum_\beta (F_\beta K_{\beta:M}^k)} \tag{13}$$

where the denominator is factored out of the summation sign. Expressing F_β using equation (7), factoring out the denominator and canceling out the common terms yields

$$\phi \sum_\alpha (\rho_\alpha S_\alpha \omega_\alpha^k) = \phi Z^k \sum_\alpha (\rho_\alpha S_\alpha) \tag{14}$$

Equation (14) is incorporated into the rate of accumulation term of equation (6), with Z^k being the primary variable. The ω_α^K are obtained from equation (11) when required for flow term computations. The singularity that occurs in the Jacobian when $\omega_\alpha^K \to 0$ and $S_\alpha \to 0$ (which is always the case for component K being an inert component in phase α) is not present in the accumulation term of the Z formulation, since it is isolated in the $\Sigma_\beta F_\beta K_{\beta:M}^K$ term, which is factored out in the Z formulation and canceled from both numerator and denominator. It should be noted that the relative permeability of the phase is equal to zero for any saturation below the residual saturation (i.e., $k_{r\alpha} = 0$ when $S_\alpha \le S_{\alpha r}$), and hence the flow term is also zero for an inert component K. This makes the Jacobian matrix (partial derivatives of flow and accumulation terms) singular for an inert component, if the ω formulation is used, causing the simulation to abort at zero saturation of the phase containing an inert component. The ω formulation therefore requires small amounts of residual inert component (to the order of $S_\alpha = 10^{-3}$) to be present throughout the domain.

For the Z formulation, however, the Jacobian at least contains the term for $\partial(Z^K \Sigma_\alpha \rho_\alpha S_\alpha)/\partial Z^K$ for inert gas component K, even if Z^K and $S_a \to 0$. The matrix is therefore guaranteed a diagonal term. Now, for $S_a \to 0$ within any grid block, the inert air component flux term is zero. Therefore only redistribution of the accumulation term occurs in that grid block due to change of the state variables during the time step. Hence

$$Z_N^K(\rho_w S_{wN} + \rho_a S_{aN} + \rho_n S_{nN}) = Z_O^K(\rho_w S_{wO} + \rho_a S_{aO} + \rho_n S_{nO}) \tag{15}$$

which can accommodate negative S_{aN} (subscripts N and O refer to new and old time step values, respectively). The penalty source term [*Forsyth*, 1994] is therefore required to give physically meaningful solutions to the discrete set of equations. This is not essential for the isothermal case; however, large changes of the state occur with temperature in a nonisothermal simulation, forcing the discretized solution into the nonphysical realm, unless controlling measures are provided.

Numerical Discretization

Spatial discretization of the governing equations is performed using upstream-weighted finite difference or finite element techniques. The discretization scheme utilizes a rectangular or orthogonal curvilinear grid with options of finite element or finite difference lattice connectivities. The Galerkin procedure is modified to incorporate upstream weighting of phase mobilities and lumping of the storage matrix [*Huyakorn et al.*, 1992a, 1994].

With fully implicit time-integration and linear brick finite elements, the improved upstream Galerkin procedure yields the following set of discretized nodal equations for (6).

$$\frac{B_i}{\Delta t}\left[\left\{\phi Z^k \sum_l (\rho_l S_l)\right\}^{t+\Delta t} - \left\{\phi Z^k \sum_l (\rho_l S_l)\right\}^{t}\right] = \sum_l \sum_{j\in\eta_i} (\rho_l \tau_l \omega_l^k)_{ups(i,j)}^{t+\Delta t} \gamma_{ij} (\psi_{lj} - \psi_{li})^{t+\Delta t} + \sum_l \sum_{j\in\eta_i'} \gamma_{ij}^D (\omega_{li}^k - \omega_{lj}^k)^{t+\Delta t} + q^k \tag{16}$$

where η_i is the set of neighbor nodes connected to node i, B_i is the nodal volume, the superscript $t + \Delta t$ denotes the current time value, the subscript $ups(i, j)$ denotes the upstream node for the nodes i, j, γ_{ij} are transmissivity coefficients computed using influence coefficient algorithms that avoid costly numerical integration, and γ_{ij}^D are the influence coefficients associated with dispersion occurring over the η_i' set of neighbor nodes such that γ_{ij}^D is nonzero. The energy equation is discretized in a similar manner.

The nonlinearity of the compositional equations is handled using a residual-based Newton-Raphson iterative technique. The primary unknowns at each iteration are selected depending on the state of the system, as was discussed previously. An underrelaxation formula that considers the maximum error of iteration is used for updating the primary variables to enhance convergence.

An automatic time stepping procedure is used which is simple but aggressive. The initial time step size Δt_1 is chosen by the user. If the nonlinear solution converges in less than a specified number of iterations (usually 5), the next time step size is automatically doubled. If convergence does not occur within a maximum specified number of iterations (usually 10), the time step is reduced by a factor of 5. The time step multiplying factor is otherwise controlled by a maximum allowable change of the variables within a time step. This time-marking procedure was found to work very well for the three-phase flow solution of *Huyakorn et al.* [1992a, 1994].

The block Orthomin solution scheme is used for solving the large, sparse systems resulting from finite element, finite difference, or hybrid discretizations of the asymmetric Newton-Raphson linearized equations. Direct solvers become cumber-

some with only a few thousand equations, and other iterative solvers such as SSOR and the strongly implicit procedure (SIP) suffer from lack of robustness, user inputs of iteration parameters, and impose restrictions on the domain discretization. The Orthomin solver used by *Huyakorn et al.* [1992a, 1994] incorporates an incomplete factorization with Orthomin acceleration algorithms of *Behie and Vinsome* [1982]. Level 1 and 0 decompositions are provided as options. The sparsity of the matrix is adjusted for the various connectivities to produce the smallest possible matrix structure. The solver has been applied to various problems over the last 3 years and has repeatedly proved its efficacy [*Panday et al.*, 1994; *Huyakorn et al.*, 1992b].

The details of matrix assembly, nonlinear treatment, underrelaxation, time marching, and matrix solution used in this study are provided by *Huyakorn et al.* [1994]. Additional enhancements have been implemented in the matrix assembly routines, since a significant portion of computation time is spent in assembly at each Newton iteration. The symmetries involved in the influence coefficients of an element have been isolated, and the contributions to a node of the influence coefficients from all adjacent elements are added. The resulting equations represent the general finite volume representations of the discretized set of governing equations. Thus a nodal assembly of the global matrix may be performed, as is done for a finite volume representation. This is more efficient than adding the contributions at a node from each of its contributing elements into the global matrix numerically, as is done in the classical finite element method. Additional computational savings have been achieved by further manipulation of constant coefficients in the discretized equations. The influence coefficients of the finite element equations and the absolute conductivity term in the flow part of the conservation equation are lumped into a "property-geometry" factor which is invariant throughout a simulation and can be assembled at the start of the simulation and saved for all nodes. During successive time steps and Newton iterations, only the nonlinearities are updated within the global matrix and right-hand side vector. Further, a columnwise pass through the Jacobian provides for efficient numerical calculation of the partial derivatives with respect to the unknowns [*Forsyth and Simpson*, 1991]. Speeding up the assembly routines is even more crucial for a compositional simulation where several components may be present than for the multiphase flow case, since a significant percentage of the simulator's time is spent in assembly.

The compositional formulation collapses automatically to the three-phase flow equations when all phases are inert, and the primary variables are P_a, S_n, and S_a for a three-phase state, as shown in Figure 1. Temperature T is always a primary variable for nonisothermal cases. Once the inert situation is identified, calculations E through K of Figure 1 and the variable substitution routines may be bypassed. In addition, generality of the equation set enables any number of fluid phases to be present in the system. If an air phase is present, an air indicator is necessary because air phase properties such as density and viscosity require special computation.

Verification Examples

The compositional formulation discussed above has been implemented into a numerical code which was tested for performance and accuracy against the decoupled formulation and against two independently developed compositional simulators: one of *Falta et al.* [1992] and the other of *Forsyth* [1994]. Several benchmark tests were also conducted against simplified solutions and analytical solutions to identify and eliminate coding errors. The NAPL flow problem discussed by *Huyakorn et al.* [1994] was first simulated with the compositional formulation, under conditions of no mass transfer (i.e., all components are inert). Results of both formulations and Newton iteration characteristics are similar. The compositional model was then verified against the compositional models of *Forsyth* [1994] and *Falta et al.* [1992]. A one-component NAPL (trichloroethylene, TCE) is injected into a 3.5 by 2.25 m rectangular domain discretized by 10 rows and 15 columns with $\Delta x = \Delta y = 0.25$ m. Prescribed pressure conditions corresponding to a water table elevation of 1.6 m and 1.5 m above the domain base were imposed, at the left and right boundaries, respectively. The system was first allowed to equilibrate from fully saturated conditions for 7 days. An air vent was provided at the top right corner where air pressure was allowed to equilibrate with atmospheric conditions. NAPL was then injected at $x = 1$ m, $y = 1.5$ m, at a rate of 0.00826 mol s^{-1} for 8460 s (0.1 day). The simulation was performed for 100 days to observe the transport of TCE in the system. Results from all codes compared very well for this simulation. The energy equation was next incorporated into the code and verified against saturated cases and analytical solutions. The compositional code with the energy equation was then benchmarked against the codes of *Forsyth* [1994] and *Falta et al.* [1992]. The same setup was used as for the TCE problem discussed earlier. For this case, however, steam was injected at $x = 1$ m, $y = 0.5$ m, at a rate of $q_w = 0.257$ mol s^{-1} and a temperature of 400 K, starting at 7.1 days (i.e., after completion of NAPL injection).

The codes used to benchmark this study are essentially different in structure and formulation. The formulation of *Forsyth* [1994] is described in category B of compositional formulations discussed earlier, and the current study employs the formulation discussed in category D earlier. The formulation of *Falta et al.* [1992] considers one component initially in each phase and solves for P_a, S_a, S_w, and T as primary variables when all phases exist, switching to P_a, X_a^c, S_w and T when NAPL phase is absent. Minute amounts of air remain in the saturated zone, and minute amounts of water remain in the unsaturated zone, by introducing a pseudopartition coefficient that goes to zero as saturation approaches zero, thus requiring no more phase switches. Disappearance of NAPL is recognized when $S_g + S_w \geq 1$, and NAPL appearance is indicated when the partial vapor pressure of the NAPL constituent ($X_a^c P_a$) is calculated as being larger than the saturated vapor pressure of the component. The pseudopartition coefficient cuts off redistribution of the accumulation term for the respective phase (air or water) in equation (16), and hence a penalty source is not required.

The code of *Forsyth* [1994] uses a finite volume discretization with assembly on triangular elements (if rectangles are provided, the code internally splits them up into triangles). The code of *Falta et al.* [1992] is an integrated finite difference code which can consider elements of all shapes as long as flow lengths, areas, and volumes are supplied to it. The present formulation uses a finite element discretization with orthogonal hexahedral elements, which is modified to allow for various nodal lattices and improved upstream weighting and to prevent negative transmissivities [*Huyakorn et al.*, 1994; *Panday et al.*, 1994]. The code of *Falta et al.* [1992] uses a direct solution technique, while the current code, and the code of *Forsyth* [1994] use Orthomin solution schemes. All codes use a fully

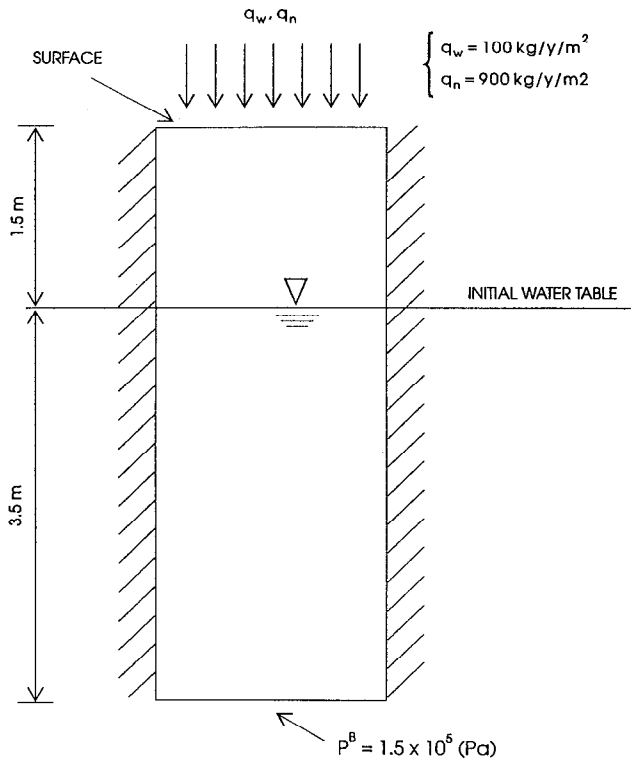

Figure 2. Geometry and boundary conditions for simulation of vertical NAPL infiltration in a soil column (example 1).

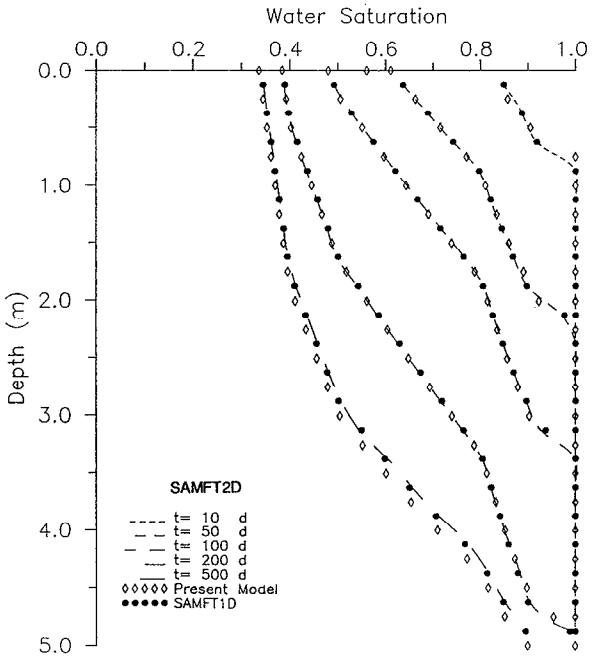

Figure 3. Predicted water saturations for simulation of vertical NAPL infiltration in a variably saturated soil column.

implicit Newton linearization as well as some form of automatic time step size selection and underrelaxation.

Vertical Immiscible Flow Example

This example problem was used by *Huyakorn et al.* [1994] to test their multiphase flow formulations. It is used here to verify performance of the compositional modules and to examine computational speed degradation resulting from solving an immiscible phase flow problem using the complex compositional procedures. A vertical, 5-m soil column (Figure 2), with an initial water table 1.5 m below the surface, was injected with 900 kg yr^{-1} m^{-2} of NAPL and 100 kg yr^{-1} m^{-2} of water at the top. The bottom boundary was assigned pressure conditions of $p_w^B = p_n^B = 1.5 \times 10^5$ Pa for both water and NAPL, representing a water-saturated condition ($S_w = 1$) until the NAPL front reaches the boundary. Water, NAPL, and soil properties used for the simulation are reported in Tables 1 and 2 of *Huyakorn et al.* [1994].

The domain was discretized in two dimensions using a rectangular grid consisting of 20 brick elements and 42 nodes, with a uniform nodal spacing of 0.25 m in the vertical direction. All mass transfer coefficients were set to zero, and the code was run in its compositional mode. Simulation results were compared with numerical solutions from the three-phase flow modules of *Huyakorn et al.* [1994] and the 1-D model of *Wu et al.* [1991]. Water and NAPL saturation profiles at various times are shown in Figures 3 and 4, respectively. The agreement between results of the various codes is excellent.

The Newton iteration behavior of the compositional model was similar to that of the multiphase flow model, both requiring a total of 101 Newton iterations for the simulation. The compositional model was, however, twice as slow as the flow model, owing to the extra computations involved in characterizing the secondary variables and in phase state checking and switching. This shows the benefit of a comprehensive simulator which can accommodate simplified formulations, where applicable. Compositional savings can be substantial in detailed site studies even for complex contamination/remediation scenarios, where preliminary flow behavior analyses and initial calibrations may be performed with the multiphase model assump-

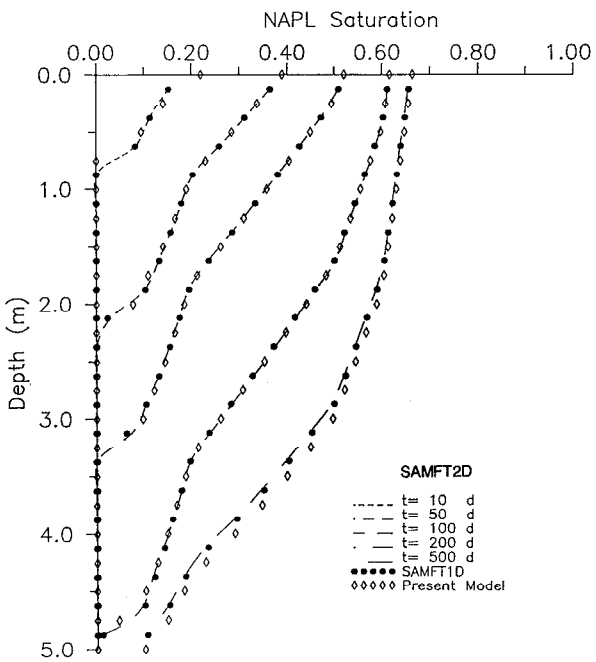

Figure 4. Predicted NAPL saturations for simulation of vertical NAPL infiltration in a variably saturated soil column.

Table 1. Simulation Times for the Various Options of Example 1 on a 33MHz PC 486

Method of Solution	Time, s
Multiphase flow approach	69
Compositional approach, three components	168
Compositional approach, six components	383
Compositional approach, six components, molar computations	396

tions. When the compositional code was allowed to recognize the inert nature of the components, the simulation time was comparable with that of the three-phase flow code. The next test of the compositional code with the same problem involved incorporating two components into every fluid phase. Every component within a phase was given the same fluid properties, so that the flow behavior of the system was the same as that for the previous simulation. Results and Newton iteration behavior for this simulation were the same as those for the previous simulations. This simulation, however, took around 5 times longer than the multiphase flow case. The number of simultaneous equations being solved here is six, as compared to three for the previous case, thus accounting for the increased solution times. The mass fractions of each of the components within a phase remained the same as the initial and boundary mass fractions supplied to the system, since mass transfer and diffusion did not occur for any component in the system. Finally, the molar computations in the code were checked with this example, by providing molar values instead of mass values. Results of this simulation were similar to the previous cases, thus confirming that obvious coding errors were eliminated. Runtime statistics of all simulations are provided in Table 1.

NAPL Spill and Subsequent Leaching and Redistribution of TCE Component Example

The domain for this problem (Figure 5) was a 3.5 m by 2.25 m rectangular cross-section, discretized using square elements with $\Delta x = \Delta y = 0.25$ m. The first stage of this laboratory-scale simulation allows for equilibration of the water table within the domain, with the hydraulic head on the left edge prescribed at 1.6 m and the head on the right edge prescribed at 1.5 m. An air vent, with constant atmospheric pressure, was placed at the top right corner. The system was allowed to equilibrate from saturated conditions for 7 days. The next stage of this simulation involved injecting NAPL at $x = 1$ m, $y = 1.5$ m, at a rate of 8.257×10^{-2} mol s^{-1} ($\equiv 7.234 \times 10^{-6}$ m^3 s^{-1}) for 0.1 day. NAPL injection was stopped for the third stage of the simulation, during which NAPL and its component were allowed to redistribute until 100 days.

Physical properties of TCE were assigned to the NAPL. Table 2 provides all chemical and soil properties of the system. The problem was simulated with and without a small amount of residual air ($S_a = 10^{-3}$) in the system, so that a direct comparison can be made with the compositional models of *Forsyth* [1994] and *Falta et al.* [1992] for the residual air saturation case. NAPL saturations at 7.1 days (at the end of injection), 13.8 days, and 100 days of simulation are shown in Figure 6. Excellent agreement is noticed between the results of all simulations. The TCE is leached out of the NAPL, and only small amounts of NAPL phase remain in the system at 100 days. Table 3 compares the total number of Newton iterations required for each of the simulations. The performance of all simulations that contain residual air in the system is similar, the differences being attributed to the different time step selection and underrelaxation parameters of the codes. However, when no residual air was allowed in the present model, the number of Newton iterations reduces significantly. Allowing

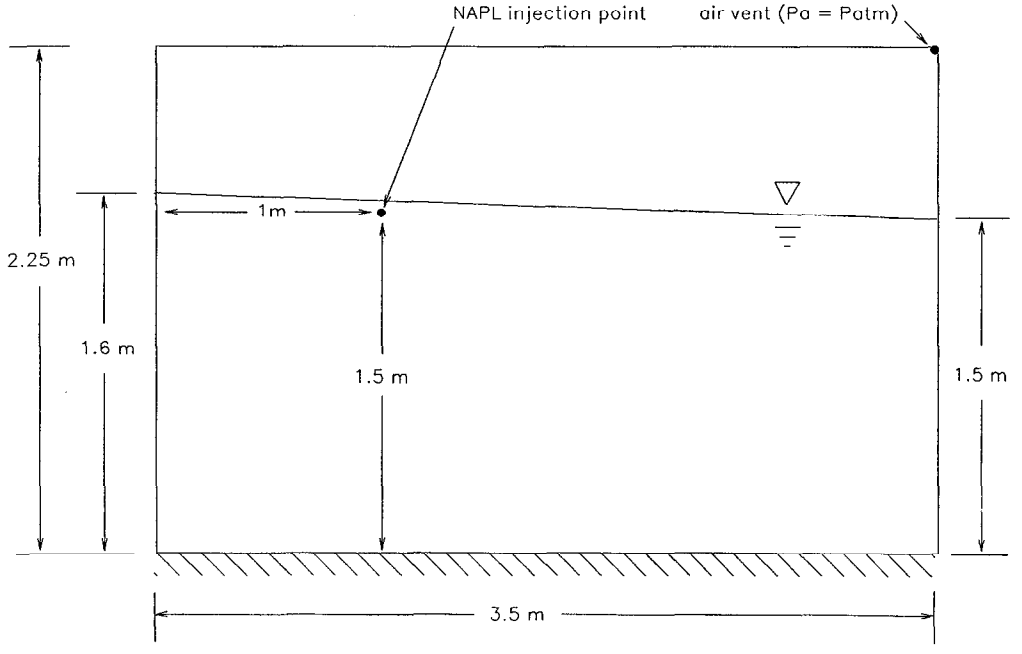

Figure 5. Geometry and boundary conditions for NAPL injection, and component redistribution problem (example 2).

Table 2. Properties of Soil and NAPL for Simulation Examples 2 and 3

Parameter	Value
Permeability k_0, m^2	0.21×10^{-11}
Porosity ϕ	0.33
Soil compressibility, Pa^{-1}	1×10^{-10}
Standard fluid molar densities	
ρ_w, mol m^{-3}	55,500
ρ_n, mol m^{-3}	11,415
ρ_a, mol m^{-3}	41.05
Component molecular weights	
M_w, kg mol^{-1}	0.018
M_n, kg mol^{-1}	0.1314
M_a, kg mol^{-1}	0.0283
Component compressibilities	
α_w, Pa^{-1}	0.43×10^{-9}
α_n, Pa^{-1}	0.3×10^{-8}
α_a, Pa^{-1}	0.1177×10^{-4}
Reference phase viscosities	
μ_w, Pa s	0.1234×10^{-2}
μ_n, Pa s	0.784×10^{-3}
μ_a, Pa s	0.2474×10^{-4}
Reference pressure P_{ref}, Pa	1×10^5
Reference temperature T_{ref}, K	293
Gravity acceleration g, m s^{-2}	9.807
Partitioning coefficients	
NAPL into air phase ($K_{n:a}$)	0.07
NAPL into water phase ($K_{w:n}$)	0.0285
Water into air phase ($K_{w:a}$)	0.010726

Soil constitutive relationships are as provided in Table 2 of *Huyakorn et al.* [1994].

for a change of state to occur and air to vanish from the system makes the problem easier, requiring half the number of computations than would be needed if residual air were present throughout the system. The formulations of *Forsyth* [1994] and *Falta et al.* [1992] require residual air to be present if the air component is inert; otherwise a breakdown in the solution with a singular Jacobian matrix occurs. In addition, switching criteria are not available for the change of state.

Several code design choices were examined with this problem. First, the mild nonlinearity of density with respect to mole fractions was allowed to lag behind one Newton iteration. The resultant number of Newton iterations required for solution was almost doubled for all cases, with a significant increase in the overall computation time. In fact, any form of approximation to the Jacobian matrix slowed down Newton convergence, and best performance was obtained when a fully implicit Jacobian matrix was built without any approximations. The nonlinearity of density with respect to mole fractions was easily resolved, usually within two Picard iterations, during calculation of the secondary variables. This computation (performed at all nodes at every Newton iteration), is cheap as compared with performing many more Newton iterations using an approximate Jacobian. A similar increase in the number of Newton iterations was noticed if a node changed state at the end of a Newton iteration and if the secondary variables were not recomputed for the new state at that node before the next iteration. Finally, constraint equation (12) was used to update Z^k for the component whose master phase saturations are the smallest. This replaces using (4) and (10) for the Z^k computation, thus ensuring that (12) always holds for the system. Otherwise, inert component phase switches slowed down convergence of the Newton iterations. This is because arrival of inert component K, and its master phase at any node, is indicated by $Z^K > 0$ at the end of any iteration. The phase switch, however, takes place with saturation of the master phase being zero ($S_M = 0$), causing a zero divide in the ω_M^K calculation (see equation F in Figure 1). When this happens, the ω_M^K is set to zero, since physically, $\omega_M^K = 0$ when $S_M = 0$ for the inert component. Now if equation K in Figure 1 were used to calculate all remaining Z^k, equation (12) would not be satisfied by the new set of variables. The zero divide is avoided for small saturations of the master phase, but the ω_M^K calculation of equation F in Figure 1 may be unreliable owing to truncation specially if the inert phase is significantly lighter than the other phases, since further truncation is introduced through equation E in Figure 1. Reverse switches cause similar situations which slow down Newton convergence. Additional techniques for smooth Newton convergence after state changes within the system were also tested with this example problem. A predictor for phase saturations after a state switch was implemented to provide smooth transitions. The scheme used provided mixed results, and the predictor was later discarded. Additional research into phase transition predictors (i.e., those that update phase pressures and ensure that all equations are satisfied) may still provide consistent schemes for enhancing Newton convergence.

Steam Injection Example

This example was selected to verify the model for nonisothermal conditions. This problem involves initial equilibration of the water table and injecting NAPL into the domain of Figure 5, just as in the previous laboratory scale simulation example. After the NAPL injection stage (7.1 days), steam was injected into the system at $x = 1$ m, $y = 0.5$ m, at a rate of 0.257 mol s^{-1} (0.4 m^3 d^{-1} water equivalent) at a temperature of 400 K. Physical properties of the system are provided in Table 2. Thermal parameters for this system are provided in the appendix. These parameters correspond to the values used in the previous example, where the isothermal temperature of the previous example is maintained at the reference temperature of 293 K. Figure 7 shows a comparison of the simulation results with results obtained by the models of *Forsyth* [1994] and *Falta et al.* [1992]. The simulation was performed with residual air ($S_{ar} = 0.001$) as well as without in order to obtain a direct comparison with *Forsyth*'s [1994] and *Falta et al.*'s [1992] codes. NAPL saturations at 7.2, 7.4, and 7.6 days of simulation are shown in Figure 7, and the temperature profiles at those times are shown in Figure 8. Results of all simulations compare well. Differences in the figures are due to the codes having selected different time steps, and the results plotted are not exactly at the same times for the different simulations. The steam front moves radially outward from its injection point, volatizing the NAPL in its path, which then condenses in cooler regions of the domain. Newton behavior of all simulations was also comparable. Forsyth's compositional model formulation required 590 Newton iterations, and Falta's formulation required 830 Newton iterations, while the present formulation required 778 iterations for the residual air saturation case and 528 iterations for the case where no residual air was present below the water table. For the comparable case of all three models (with a residual air saturation of 0.001) the formulation of *Forsyth* [1994] performed the best, with a similar Newton performance between *Falta et al.*'s [1992] formulation and our current formulation. The burden on our formulation was eased, however, when phase switches were allowed

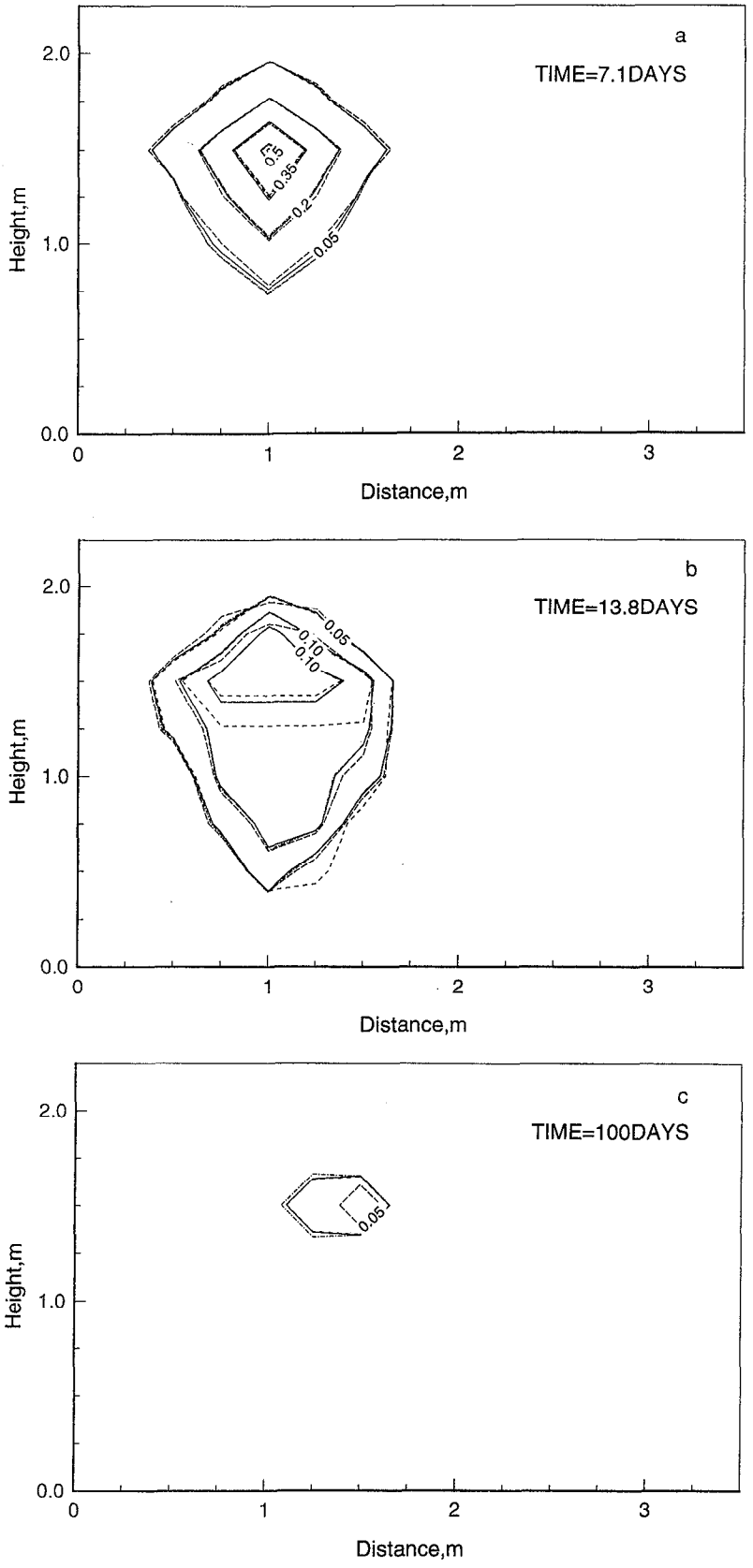

Figure 6. NAPL saturation distributions at (a) 7.1 days, (b) 13.8 days, and (c) 100 days for the NAPL spill and subsequent leaching example. Short-dashed lines, present model with no residual air; long-dashed lines, present model with residual air $S_{ar} = 0.001$; solid lines, *Forsyth* [1994] model; dash-dot line, *Falta et al.* [1992] model.

Table 3. Comparison of Computational Burden for the Simulations of Example 2

Newton Iterations Required	Present Model		Model of *Forsyth* [1994]	Model of *Falta et al.* [1992]
	With Residual Air	Without Residual Air		
Water equilibration stage (0–7 days)	47	47	51	66
Oil injection stage (7–7.1 days)	38	38	33	51
Redistribution stage (7.1–100 days)	742	294	793	909
Total	827	379	877	1026

(without residual air saturations), and the formulation performance was comparable to that of Forsyth.

A critical parameter controlling Newton iteration behavior was the penalty source term. If the penalty source term were not implemented, the solution proceeded to give negative saturations and large negative mole fractions. The problem was not alleviated by phase switching for negative saturations, since the solution would proceed along the lines of providing zero saturation for the inert component's master phase, which was obviously present (due to equilibrium temperature pressure conditions), and meaningless mole fractions resulted. Enforcing a penalty source resolved that problem. A discussion of the controlling mechanisms of a penalty source term and its significance to the accuracy of solution is provided by *Forsyth* [1994]. Choice of a penalty source term, however, affected Newton convergence behavior. The penalty source used in this model is

$$q^{*K} = f \frac{|\omega_\alpha^K|}{\Delta t} \max (S_n\rho_n, S_w\rho_w, S_a\rho_a) \qquad (17)$$

where f is a factor (10^{-3} in this case) which can be adjusted for robustness. In calculating the Jacobian, the penalty source is not implemented on a shifted variable if it was not required for the unshifted calculations. This choice of penalty source provided some form of consistent Newton behavior. For example, if $(\omega_\alpha^K)^2$ were used in place of $|\omega_\alpha^K|$ in the penalty source equation, the no-residual gas case converged in 426 iterations, but the residual gas case took 920 iterations to converge. Similar erratic behavior of the Newton iteration count occurred when the term $[\max (S_n\rho_n, S_w\rho_w, S_a\rho_a)]$ is replaced by $[S_n\rho_n + S_w\rho_w + S_a\rho_a]$ in the penalty source term. Further research is required for optimal selection of a penalty source term which is not sensitive to the state of the system in terms of the Newton iteration count. It should be noted that this example problem is a computationally difficult case, with all kinds of vaporization and condensation occurring throughout the system. The model of *Forsyth* [1994] exhibited difficulty proceeding beyond 7.6 days. The current model did not have this great difficulty, and the simulation proceeded in a stable though sluggish fashion beyond 7.6 days, as did the model of *Falta et al.* [1992].

The phase-switching criteria were also modified for the thermal case. As was mentioned earlier, a possible solution to the discrete set of equations is to yield negative saturations. If this solution was accompanied by negative mole fractions of components in the phase with a negative saturation and $\Sigma_k |\omega^k| > 1$ for that phase, it would indicate that the phase is actually still present and that imposing the penalty source term would resolve the situation in the next iteration. Therefore if at an iteration $S_\alpha < 0$, a check was also made on $\Sigma_k |\omega_\alpha^k| \leq 1$, before the state was switched at that location. This is the physically correct state-switching criterion, and switching with any other criteria (e.g., if only $S_\alpha < 0$ was the criterion for switching) provided poorer Newton convergence.

Conclusions

A compositional model was developed and benchmarked against a multiphase flow model using a 1-D NAPL infiltration example. Model verification and assessment of computational performance of the compositional routines were conducted next, using a NAPL injection and component redistribution example for the isothermal case and a steam displacement problem for the nonisothermal case. Both examples are challenging problems for a numerical simulator, since numerous nonlinear processes occur in the system. The selected examples provide a good basis for examining techniques of increasing robustness of the simulator even further. The test problems serve to demonstrate the simulation capability and accuracy of the three models used, which differ not only in basic structure but also in the mathematical formulation, spatial discretization approximation, and numerical implementation. The commonality of the tested codes is that they may be used to represent the same physical problem and that they all use full Newton iterations for linearization of the equations, therefore enabling a robustness comparison by counting the Newton iterations. Another notable point is that for a similar problem setup (i.e., with a residual air saturation of 0.001), all formulations gave similar Newton performance. It would be interesting to examine the Newton convergence behavior of the compositional formulation discussed in category A, since it would indicate if additional robustness were possible with a different set of primary variables, selected from the same total set of variables.

Two computational processes have been identified, which degrade the simulation performance for tough problems. First, a phase switch jolts the system into possibly requiring more Newton iterations. This is because the primary variables are switched for the new state, but the starting values for the next iteration are not completely consistent with the new state of the system. It should be noted that the compositional scheme employed in this work minimizes the number of primary variables that are switched; however, the largest jolts seem to be due to the switching of Z^k and S_α when a phase state change occurs. This is deduced from the fact that Forsyth's formulation incorporates the additional switches of ω_α^k from one phase to another, while the current formulation does not require

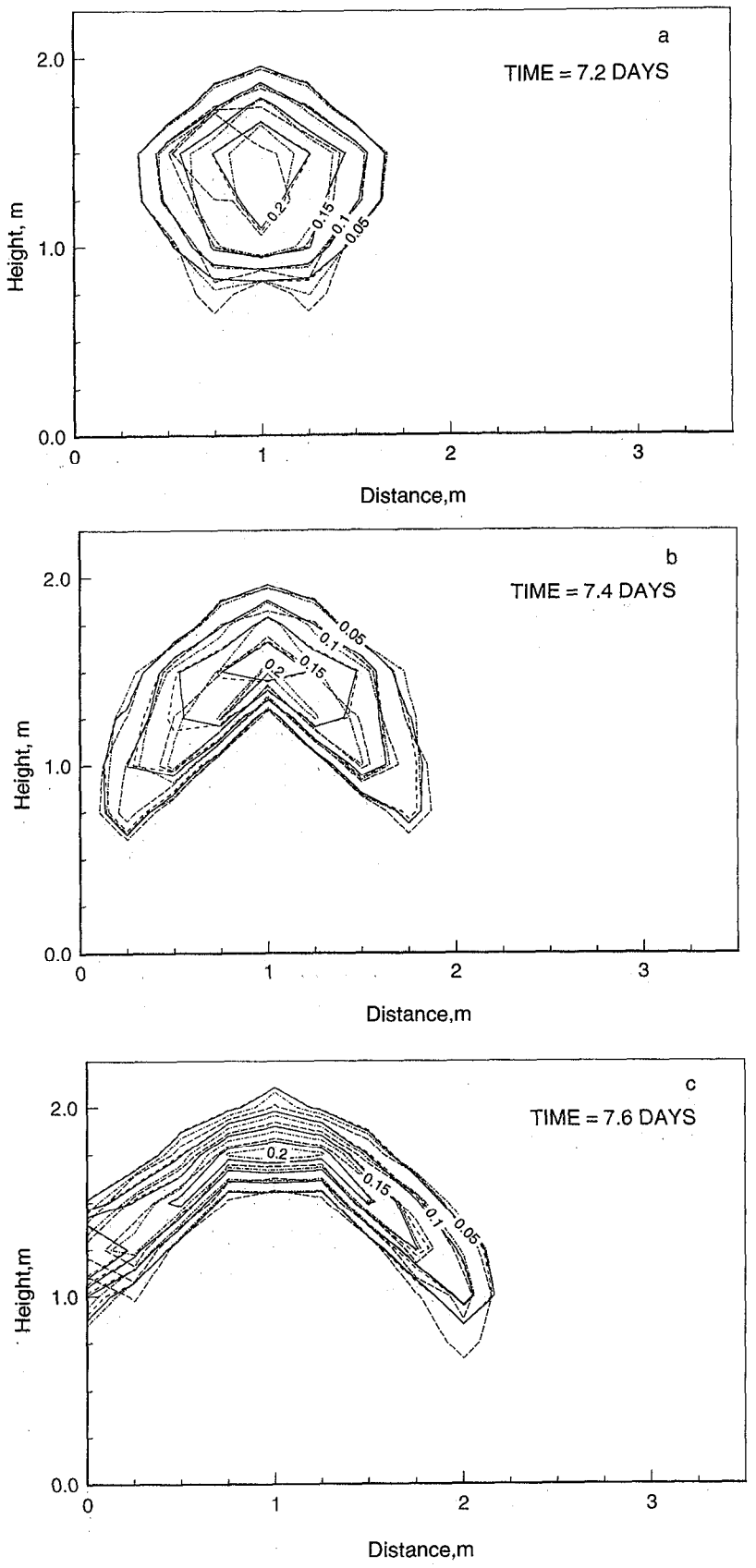

Figure 7. NAPL saturation distributions at (a) 7.2 days, (b) 7.4 days, and (c) 7.6 days for the steam injection example. Short-dashed lines, present model with no residual air; long-dashed lines, present model with residual air $S_{ar} = 0.001$; solid lines, *Forsyth* [1994] model; dash-dot line, *Falta et al.* [1992] model.

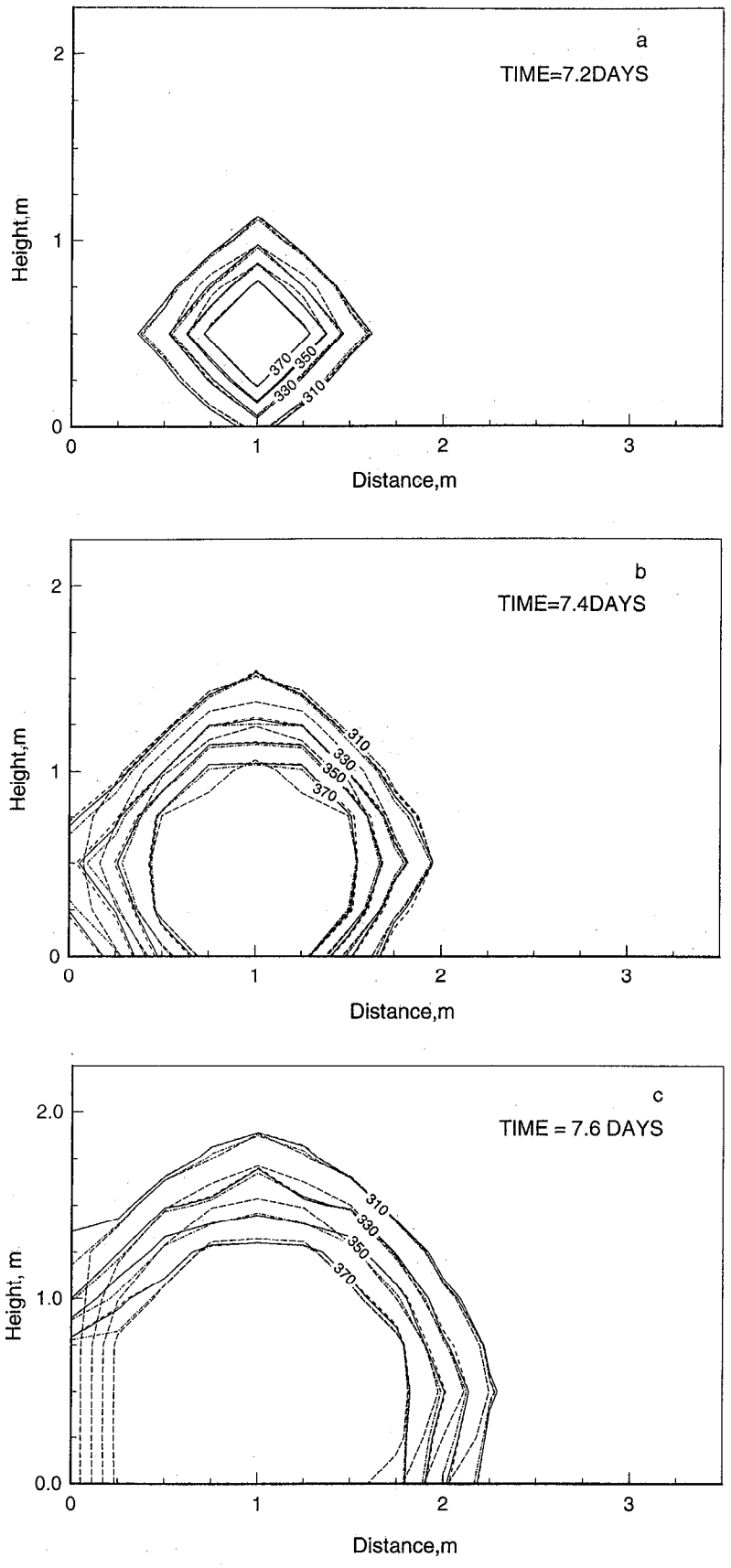

Figure 8. Temperature profiles at (a) 7.2 days, (b) 7.4 days, and (c) 7.6 days for the steam injection example. Short-dashed lines, present model with no residual air; long-dashed lines, present model with residual air $S_{ar} = 0.001$; solid lines, *Forsyth* [1994] model; dash-dot line, *Falta et al.* [1992] model.

these switches; however, both formulations have similar Newton behavior for a similar problem setup. Predictor techniques, which estimate Z^k or S_α at a phase switch, provided mixed results, since now the pressure-saturation state of the system is imbalanced. Additional research on predictor techniques that update all variables for the new state would prove useful in further increasing the robustness of the simulator. The second process that was identified as a crucial potential degrader to simulation performance is choice of the penalty source term in thermal simulations with inert components. If too much penalty source was introduced, the simulator took more Newton iterations to rid itself of the excess component introduced. Too small a penalty source proved ineffective in controlling the negative mole fractions. A deeper understanding of the nature of the Jacobian matrix when a penalty source is applied is required to provide more robust expressions for the penalty source term.

A nonisothermal compositional formulation has been implemented into a comprehensive numerical model. Various compositional schemes were first examined to identify advantages and pitfalls in solving groundwater-contamination-related problems. The compositional formulation developed in this work proved to be more robust than the other recently developed formulations against which it was tested for the isothermal case. Furthermore, the proposed model was at least as robust as the previous models for the nonisothermal case. A further advantage of the present scheme is its complete generality in simulation for all cases, from insoluble/nonvolatile components to components with large equilibrium mass transfer coefficients.

Appendix: Thermal-Related Properties Required for Steam Injection Simulation of Example 3

Liquid densities

$$\rho_l = \frac{(1 + C_l(p_l - p^*) - E_l(T - T^*)}{\sum_k \max(O, \omega_l^k)/\rho_k^*} \qquad l = w, n$$

for liquid phase densities ρ_l, where p^* and T^* are reference pressure and temperature, respectively; C_l is compressibility ($C_w = 4.3 \times 10^{-8}$ Pa^{-1}; $C_n = 3 \times 10^{-7}$ Pa^{-1}); E_l is thermal expansion ($E_l = 0$, $l = w, n$), and ρ_k^* are standard component molar densities.

Gas density

$$\rho_g = p_g/RT$$

where R is universal gas constant.

Contaminant equilibrium ratios

$$K_{g:\beta}^k = 1000 \exp\left[a_{g\beta}^k - \frac{b_{g\beta}^k}{T - C_{g\beta}^k}\right] \Big/ p_g \qquad \beta = n, w$$

where k are components of NAPL phase; $a_{g\beta}^k$, $b_{g\beta}^k$, $c_{g\beta}^k$ are constants,

$$a_{gn}^n = 9.28 \qquad b_{gn}^n = 462 \qquad c_{gn}^n = 230 \text{ K}$$

$$a_{gw}^n = 15.14 \qquad b_{gw}^n = b_{gn}^n \qquad c_{gw}^n = c_{gn}^n$$

Water equilibrium ratio

$$K_{g:w}^w = 1000 a_{gw}^w (T - c_{gw}^w)^{b_{gw}^w}/pg$$

where

$$a_{gw}^w = 0.8777 \times 10^{-8} \qquad b_{gw}^w = 4.76 \qquad c_{gw}^w = 243 \text{ K}$$

Enthalpies

$$h_g^k = C_l^k(T_s^k - T^*) + h_{\text{lat}}^k + C_g^k(T - T_s^k)$$

$$h_l^k = C_l^k(T - T^*)$$

$$h_g^g = C_g^g(T - T^*)$$

where h_g^k is enthalpy of component k in gas phase, h_l^k is enthalpy of component k in liquid phase, C_l^k and C_g^k are heat capacities of liquid and gaseous components k, h_{lat}^k is latent heat of vaporization of component k, $h_{\text{lat}}^k = h_{vp}^k(T_{cr}^k - T_s^k)^{ev}$, T_s^k is the steam temperature of component k (obtained by solving $K_{g:\alpha}^k = 1$), T_{cr}^k = critical temperature, and ev is a constant.

$$C_l^w = 75.4 \text{ J mol}^{-1} \text{ K}^{-1} \qquad C_g^w = 30.5 \text{ J mol}^{-1} \text{ K}^{-1}$$

$$C_l^n = 105 \text{ J mol}^{-1} \text{ K}^{-1}$$

$$C_g^n = 30 \text{ J mol}^{-1} \text{ K}^{-1} \qquad C_g^a = 30.5 \text{ J mol}^{-1} \text{ K}^{-1}$$

$$h_{vp}^w = 4810 \text{ J mol}^{-1}$$

$$h_{vp}^n = 4360 \text{ J mol}^{-1} \qquad T_{cr}^w = 647.3 \text{ K}$$

$$T_{cr}^n = 571 \text{ K} \qquad ev = 0.38$$

Phase enthalpies are computed from component enthalpies using $h_\alpha = \Sigma_k h_\alpha^k \omega_\alpha^k$.

Internal energy

$$U_\alpha = h_\alpha - p_\alpha/\rho_\alpha \qquad U_s = \frac{H_s}{\rho_s}(T - T^*)$$

where U_s is the internal energy of soil solids and H_s is the heat capacity of soil solids.

$$H_s/\rho_s = 2.3 \times 10^6 \text{ J m}^{-3} \text{ K}^{-1}$$

Thermal conductivity

$$\Lambda_{ij} = 1.1574 \text{ J m}^{-1} \text{ K}^{-1} \text{ s}^{-1}$$

Viscosities

$$\mu_w = \frac{8.64 \times 10^{-2}}{12.1 + 2.88T' + 7.78 \times 10^{-4}(T')^2}$$

where T' is the temperature in degrees Celsius,

$$\mu_a = 8.64 \times 10^{-6}(1.574 + 0.0044T')$$

and $\mu_n = \mu_n(T)$, interpolated from a table of μ_n versus T, below.

Temperature, K	μ, Pa s
273	0.9×10^{-3}
373	0.32×10^{-3}
673	0.1×10^{-3}

Acknowledgment. This work was funded in part by NSF-SBIR award 111-9261292.

References

Abriola, L. M., and G. F. Pinder, A multiphase approach to the modeling of porous media contamination by organic compounds, 1, Equation development, *Water Resour. Res.*, *21*(1), 11–18, 1985.

Adenekan, A. E., T. W. Patzek, and K. Pruess, Modeling of multiphase transport of multicomponent organic contaminants and heat in the subsurface: Numerical model formulation, *Water Resour. Res.*, *29*(11), 3727–3740, 1993.

Aziz, K., and A. Settari, *Petroleum Reservoir Simulation*, Applied Science Publishers, London, 1979.

Behie, A., and P. K. W. Vinsome, Block iterative methods for fully implicit reservoir simulation, *Soc. Pet. Eng. J.*, *22*, 658–666, 1982.

Chien, M. C. H., H. E. Yardumain, E. Y. Chung, and W. W. Todd, The formulation of a thermal simulation model in a vectorized general purpose reservoir simulator, paper presented at the SPE Symposium on Reservoir Simulator, Soc. of Pet. Eng., Houston, Tex., 1989.

Coats, K. H., In-situ combustion model, *Soc. Pet. Eng. J.*, *20*, 533–554, 1980.

Corapcioglu, M. Y., and A. L. Baehr, A compositional multiphase model for groundwater contamination by petroleum products, 1, Theoretical considerations, *Water Resour. Res.*, *23*(1), 191–200, 1987.

Corapcioglu, M. Y., and S. Panday, Compositional multiphase flow models, *Adv. Porous Media*, *1*, 1–59, 1991.

Falta, R. W., K. Pruess, I. Javandel, and P. A. Witherspoon, Numerical modeling of steam injection for the removal of nonaqueous phase liquids from the subsurface, 1, Numerical formulation, *Water Resour. Res.*, *28*(2), 443–449, 1992.

Faust, C. R., Transport of immiscible fluids within and below the unsaturated zone: A numerical model, *Water Resour. Res.*, *21*(4), 587–596, 1985.

Forsyth, P. A., Adaptive implicit criteria for two-phase flow with gravity and capillary pressure, *SIAM J. Sci. Stat. Comput.*, *10*(2), 227–252, 1989.

Forsyth, P. A., A control volume finite element approach to NAPL groundwater contamination, *SIAM J. Sci. Stat. Comput.*, *12*(5), 1029–1057, 1991.

Forsyth, P. A., A positivity preserving method for simulation of steam injection for NAPL site remediation, *Adv. Water Resour.*, *16*, 351–370, 1994.

Forsyth, P. A., and B. Y. Shao, Numerical simulation of gas venting for NAPL site remediation, *Adv. Water Resour.*, *14*, 354–367, 1991.

Forsyth, P. A., and R. B. Simpson, A two-phase, two-component model for natural convection in a porous medium, *Int. J. Numer. Methods Fluids*, *12*, 655–682, 1991.

Huyakorn, P. S., S. Panday, and Y. S. Wu, SAMFT2D—Single and multiphase flow and transport in 2 dimensions, version 1.0, code documentation, Los Alamos Natl. Lab., Los Alamos, N. Mex., 1992a.

Huyakorn, P. S., Y. S. Wu, and S. Panday, A comprehensive three-dimensional numerical model for predicting the transport and fate of petroleum hydrocarbons in the subsurface, in *Groundwater Management Book 14, Proceedings of the 1992 Petroleum Hydrocarbons and Organic Chemicals in Groundwater Conference,* pp. 239–253, Water Well Journal Publishing, Dublin, Ohio, 1992b.

Huyakorn, P. S., S. Panday, and Y. S. Wu, A three-dimensional multiphase flow model for assessing NAPL contamination in porous and fractured media, I, Formulation, *J. Contam. Hydrol.*, *16*, 109–130, 1994.

Kaluarachchi, J. J., and J. C. Parker, An efficient finite element method for modeling multiphase flow, *Water Resour. Res.*, *25*, 43–54, 1989.

Nghiem, L. X., A new approach to quasi-Newton methods with application to compositional modeling, paper presented at the SPE Reservoir Simulation Symposium, Soc. of Pet. Eng., San Francisco, Calif., 1983.

Panday, S., and M. Y. Corapcioglu, Reservoir transport equations by compositional approach, *Transp. Porous Media*, *4*, 369–393, 1989.

Panday, S., and M. Y. Corapcioglu, Theory of phase-separate multicomponent contamination in frozen soils, *J. Contam. Hydrol.*, *16*, 235–269, 1994.

Panday, S., Y.-S. Wu, and P. S. Huyakorn, A three-dimensional multiphase flow model for assessing NAPL contamination in porous and fractured media, II, Porous medium simulation examples, *J. Contam. Hydrol.*, *16*, 131–156, 1994.

Reeves, H. W., and L. M. Abriola, A decoupled approach to the simulation of flow and transport of non-aqueous organic phase contaminants through porous media, in *Proceedings VII International Conference on Computational Methods in Water Resources*, vol. 1, *Modeling Surface and Subsurface Flows, Develop. Water Sci.*, *35*, edited by M. A. Celia et al., pp. 147–152, Elsevier, New York, 1988.

Sleep, B. E., and J. F. Sykes, Compositional simulation of groundwater contamination by organic compounds, 1, Model development and verification, *Water Resour. Res.*, *29*(6), 1697–1708, 1993.

Stone, H. L., Estimation of three-phase relative permeability and residual oil data, *J. Can. Pet. Technol.*, *12*, 53–61, 1973.

Todd, M. R., P. M. O'Dell, and G. J. Hirasaki, Methods for increased accuracy in reservoir simulators, *Soc. Pet. Eng. J.*, *12*, 515–530, 1972.

Wu, Y.-S., P. S. Huyakorn, S. Panday, N. S. Park, and J. B. Kool, SAMFT1D—Single-phase and multiphase flow and transport in 1 dimension, version 2.0, code documentation, Los Alamos Natl. Lab., Los Alamos, N. Mex., 1991.

R. W. Falta, Department of Geological Sciences, Clemson University, Clemson, SC 29631.

P. A. Forsyth, Department of Computer Sciences, University of Waterloo, Waterloo, Ontario, Canada N2L 3G1.

P. S. Huyakorn, S. Panday, and Y.-S. Wu, HydroGeoLogic, Inc., 1165 Herndon Parkway, Suite 900, Herndon, VA 22070. (e-mail: hgl@access.digex.com)

(Received April 23, 1994; revised December 8, 1994;
accepted December 12, 1994.)